PERFORMANCE ASSESSMENT OF SPACE-BASED OPTICAL NETWORKS FOR DEBRIS OBSERVATION AND TRACKING IN LEO

Antonio D'Anniballe[(1)], **Leonard Felicetti**[(2)], **and Stephen Hobbs**[(2)]

[(1)]*Cranfield University, MK43 0AL, United Kingdom, antonio.danniballe@cranfield.ac.uk*
[(2)]*Cranfield University, MK43 0AL, United Kingdom*

ABSTRACT

Space situational awareness of the Low Earth Orbit (LEO) region is today mostly enabled by ground networks of radar sensors. The main disadvantage of such systems is that they provide unbalanced coverage favouring the Northern hemisphere while also having difficulties observing targets below a few centimetres, including potentially dangerous space debris. Some of these difficulties could be overcome using space-based observation platforms. However, even under the hypothesis of using small satellites, the high cost of space launches makes the cost-benefit analysis of such a scenario uncertain. This work aims to analyse the maximum expected performance of space-based surveillance networks. This is done by retrieving the time evolution and the parametric dependencies for different performance metrics, such as the system coverage and expected target revisit time. Multiple constellation architectures are analysed based on their coverage, scalability and distributions of the expected revisit time for targets of various sizes in LEO. The resulting analysis fills a gap in the performance estimation of space-based optical networks and enables cost-benefit analyses to enhance current space situational awareness systems. Future actors can use these results to quantitatively relate the expected marginal increase of the whole surveillance and tracking system performance to the investments in networks of space-based optical systems.

Keywords: Space-based sensing, Constellation design, Space sustainability, Space debris tracking.

1. INTRODUCTION

The number of anthropogenic objects in the near-Earth space has increased dramatically in the past few years, raising the potential for collision risk [1]. To guarantee the long-term sustainability of the space environment, it is paramount to guarantee reliable conjunction alert to readily plan collision avoidance manoeuvres. To do this, timely, frequent, and accurate measurements of the state of the orbiting objects are needed for producing usable estimates. Most surveillance networks, systems aiming at achieving exactly this goal, are systems of ground sensors, mostly radars in the case of Low-Earth Orbit (LEO) objects. The main disadvantage of these systems is that they cannot be located anywhere on Earth, with the resulting strong geographic constraints harming the time availability of measurements.

In recent times, space-based optical sensors have been tested for GEO observation [2]. Interest in the concept has also been shown by ESA as a mean to observe small-size debris through the VISDOMS mission [3], increasing the reliability of debris models to support space sustainability. Recent research targeting space-based surveillance networks has investigated how to set up a coordinated space-based system [4], how to design the supporting subsystem [5], how to engineer the supporting attitude control schemes [6] and how to optimally design large constellations for space-based surveillance [7], among others.

In this paper, we develop a general purpose methodology for retrieving the tracking performance of a network of space-to-space optical surveillance satellites. By developing quantitative metrics with low computational cost, we test multiple architectures and tracking strategies to retrieve the upper bound and expected performances of this class of systems. In Section 2, we list a series of visibility conditions for an orbiting object as observed by an optical sensor in space as a baseline for our performance assessment method. We subsequently list up some baseline constellation architectures that we are confident being close to the Pareto front of the system class based on past results available in the literature. We then explain the simulation setup used to test the performance metrics, detailing how it is used to test the performance of the different architectures and tracking strategies. Section 3 lists the performance results for the different constellation architectures and tracking strategies, discussing performance drivers and parametric dependencies. Section 4 summarizes the main takeaways from the work, stressing how it validates the mission concept as a potential alternative to ground-based surveillance and the impact it has for future evaluation of similar systems.

2. METHODOLOGY

This section contains a description of the objectives of the paper, the corresponding performance metrics analysed in numerical simulations, and the details of the numerical implementation. Our goal is to find the maximum expected performance of a space-based surveillance network. The class of missions we refer to are constellations of small satellites tasked with tracking the population of anthropogenic objects in LEO of size above 10 cm using optical sensors. Based on currently investigated solutions [8], we consider the case of a constellation with size 20 to 30 observing satellites to guarantee compliance with technological feasibility. In the process, we define performance metrics that can be tested for in a numerical simulation environment. We use the resulting performance assessment method to analyse three different architectures that are deemed close to optimal based on existing literature. By comparing their performance, we obtain a quantitative estimate of the maximum achievable space-based surveillance performance. The methodology builds upon two core ideas:

- Based on results in past literature, we have good reasons to believe symmetric and/or Sun-Synchronous constellations are close to the Pareto front of the system class we are analysing, and therefore we may neglect all other network configurations, greatly reducing the dimensionality of the problem.
- We can decouple the design of the constellation architecture from the design of the tracking strategy by noticing that the volume spanned by the field-of-view (FOV) of the sensor is a subset of that spanned by field-of-regard (FOR), and therefore neglecting the condition that a target object must lie within the FOV yields an upper bound on the constellation performance. Tracking can be tested later, coupling it only to the architecture with the highest performance upper bound.

Exploiting these facts, the resulting methodology is a fast way to quantitatively compare a vast class of systems in the preliminary evaluation and design of space-based surveillance constellations.

2.1. Visibility conditions

The first step in the development of the performance assessment model is to understand when a target would be visible to a space-based observer. We have four different conditions (see Fig. 1):

1. **Shadowing condition**: It checks whether the target is outside (true) or inside (false) the Earth's shadow. It is independent of the observer's position. A target that is shadowed isn't reached by light and therefore can't scatter it back.

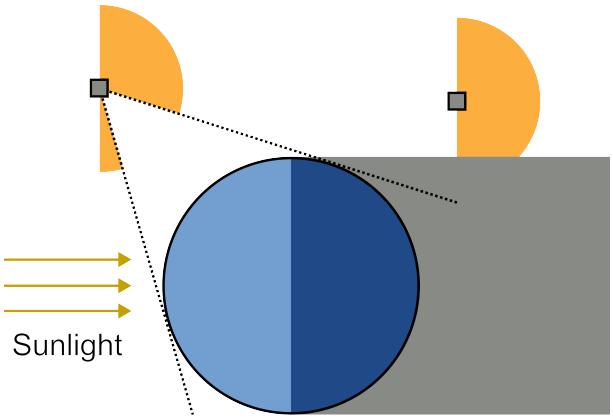

Figure 1: Illustration of the field-of-regard under visibility conditions 1-3

2. **Horizon condition**: It checks whether the Earth is occupying (false) or not (true) the target's background view (or whether the Earth is obstructing the target's view) as seen by the observer satellite. A target that has a black background produces an optical signal that is not affected by a high background noise, and therefore needs lower detection capabilities.
3. **Limiting magnitude condition**: It checks whether the apparent magnitude of the target is below (true) or above (false) the limiting magnitude of the observing sensor. A target that is too far away or in a bad geometry won't scatter back enough light to be detectable by the sensor. This is a case of high apparent magnitude. To compute the apparent magnitude, we use the model by Hejduk [9]:

$$M_v = M_s - 2.5 \log \left[A \rho F(\Phi) \right] + 5 \log r \qquad (1)$$

where M_s is the apparent magnitude of the Sun, A is the cross-sectional area of the target, ρ is the reflectivity of the target (assumed to be 0.2 [10]), r is the distance of the target from the observer, $F(\Phi)$ is the phase function as a function of the phase angle Φ (see Fig. 2), assumed to be a mixture of a diffusive and a specular component. In this paper we assume the limiting magnitude of the sensor is +12 [7].

4. **Field-of-view (FOV) condition**: It checks whether the target is within (true) or outside (false) the field-of-view of the observing sensor. For a conical field of view, this condition is equivalent to:

$$\arccos\left(\frac{\mathbf{r} \cdot \mathbf{e}_p}{r}\right) < \frac{\beta_{FOV}}{2} \qquad (2)$$

where r is the distance of the target from the observer, $\mathbf{e}_p$ is the pointing direction, and β_{FOV} is the field-of-view angle of the sensor. In this paper, we assume β_{FOV} = 5°.

If a target satisfies conditions 1 to 3, we say it belongs to the **field-of-regard (FOR)** of the sensor. For a fixed

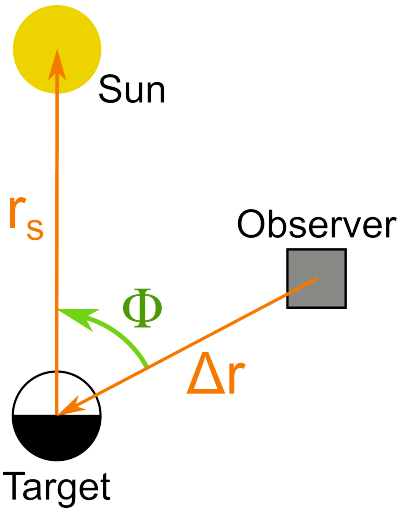

Figure 2: Illustration of the phase angle Φ

target size, the FOR is the percentage of volume that is potentially observable by the sensor. To make an actual observation, the sensor must point in the direction of the target to satisfy condition 4. Since FOV $\subseteq$ FOR, using only conditions 1 to 3 yields an upper bound for the constellation performance. Ultimately, we obtain a visibility function $f_v(\mathbf{r}_s(t), \mathbf{r}_t(t), D_t)$, where $\mathbf{r}_s$ is the observer satellite position vector, $\mathbf{r}_t$ is the target position vector, D_t is the target equivalent diameter. The visibility function can take values $\{0, 1\}$.

2.2. Constellation architectures

We consider three different types of constellation architectures (see Fig. 3):

1. **Single orbit Sun-Synchronous**: Satellites are placed at the same angular distance on the same orbit, which is Sun-Synchronous (SSO). In particular, the RAAN precession due to the Earth-oblateness effect is such that it preserves the same geometry with respect to the Sun. This constant illumination condition should intuitively be close to optimal as it guarantees an semi-constant performance throughout the year [5]. The orbital plane is set to be almost perpendicular to the Sun direction, so that the constellation does not pass through the part of the sky shadowed by the Earth, where it would yield no measurements.

2. **Double orbit Sun-Synchronous**: Two SSO orbits with the RAAN shifted by 180°. This reduces overlapping of the FORs and therefore increases satellite capacity: we need more satellites before a diminishing return in performance, possibly improving scalability.

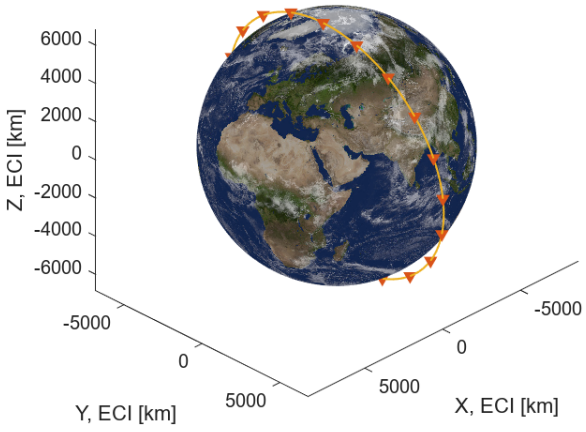

(a) Single SSO

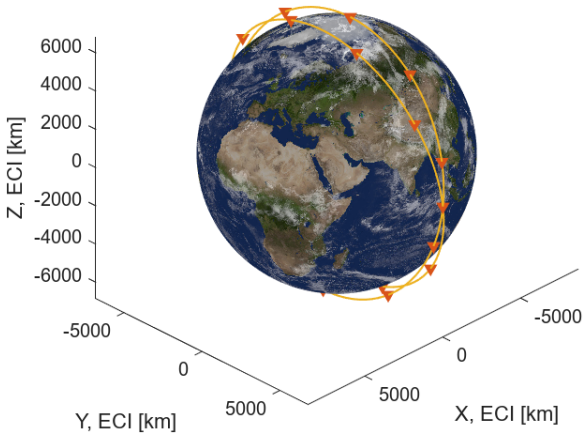

(b) Double SSO

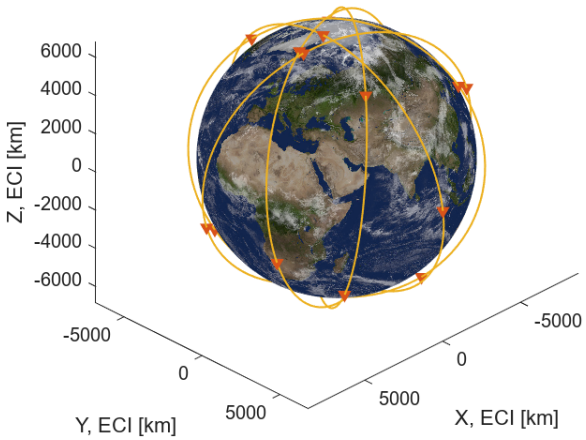

(c) Walker

Figure 3: Analysed constellation architectures

3. **Walker-Delta constellation**: Walker constellations are radially symmetric constellations composed of orbits of constant inclinations containing the same number of satellites [11]. The architecture optimizes the distribution of satellites to guarantee more uniform coverage, but can suffer from performance degrading RAAN precession depending on the chosen orbital inclination. We assume a Walker 75°: 20/5/1 as it should maximise performance based on past re-

search [7].

To guarantee the sustainability of operations, we set the maximum satellite lifetime after failure to be 5 years, which is compatible with an orbit altitude of 460 km [7]. This corresponds to inclinations of 97.3° for the two SSO architectures.

2.3. Tracking strategies

Once the optimal architecture is fixed, the performance is still affected by the chosen tracking strategy. A tracking strategy is a sequential set of pointing actions for the observer satellites. The way we decide how the observer searches and points to targets may affect how many targets we observe or for how long, among others. In this work we only consider tracking strategies that are memoryless, i.e. do not take into account how past decisions affected performance, and uncooperative, i.e. each observer optimizes its own tracking strategy disregarding the action of other observers. We consider four tracking strategies:

1. **Radial**: Pointing direction is fixed opposite to nadir, along the direction of the observer position vector.
2. **Along-track**: Pointing direction is fixed in the direction of the motion of the observer, aligned with its velocity vector.
3. **Cross-track**: Pointing direction is fixed perpendicular to the orbital plane, aligned with the angular momentum vector.
4. **Greedy**: At each timestep, the pointing direction is changed as to maximise the number of observed targets. We assume a perfect model and a maximum slew rate of 1 deg/s.

2.4. Performance metrics

To allow the comparison of different architectures and tracking strategies we need quantitative metrics that are related to surveillance and tracking performance. We can distinguish two main categories of metrics, depending on whether targets are considered to be static (fixed points in space) or dynamic (orbiting debris or satellites).

1. **Static metrics**: Computed with respect to the target distribution in space, disregarding the dynamics of the targets. Targets are point in space and not dynamically moving debris. These kind of metrics give an indication of how good the geometry of the constellation is in reaching any subset of observable space. Such metrics include:
   (a) **Instantaneous coverage**: Percentage of the observed volume weighted over the target population at any one time. It can be written as:
   $$\mathrm{cov}_N(t) = \int_{\mathcal{T}(t)} f_{v,N}(\mathbf{r}_t, D_t) d\mathbf{r}_t dD_t \quad (3)$$
   where $\mathcal{T}(t)$ is the target population set at time t and $f_{v,N}$ is the N-fold visibility function, i.e. the function that takes 1 if there are at least N sensors satisfying f_v for the given target, and 0 otherwise. We are interested in $N > 1$ because having redundancies in the observation opportunities increases the size of the effective action set. In particular, more subsets of the actions yield good tracking, and therefore it is easier to search for a good tracking policy.
   (b) **Yearly coverage variability**: Coverage variation over one year. Useful to understand the effects of the Sun position on the constellation performance. We expect seasonal effects as polar caps have opposite illuminations during solstices.
   (c) **Coverage scalability**: Coverage change for additional observer satellites. It is used to understand whether the architecture scales well and can be effective when investing in a mission upgrade.
2. **Dynamic metrics**: Computed with respect to actual targets sampled from the target distribution for a given time window. They more closely resemble the performance of tracking operations since they follow the targets in their orbits. In particular, static performance gives aggregate metrics over the target distribution, but gives no information on how coverage is distributed among targets. In particular, some orbit may be very well tracked for most of the time, while others may be badly tracked. The main drawback is the dependence on the time window. If the time window is too short, results may not be significant. If it is too long, it may take too long to compute them. The significant object in dynamic metrics is the **track**, a set:
   $$T^k_{t_0,N_t} = \{\theta^k(t_0), \ldots, \theta^k(t_0 + N_t\Delta t)\} \quad (4)$$
   of subsequent measurements without gaps of length N_t for a given target k.
   (a) **Percentage of observed population** (within half a orbital period): Percentage of the target population that has at least one track within one half orbital period. This represents the percentage of population that can be reliably tracked, as tracks that are separated by more than one half orbital periods may yield difficulties in object association [12].
   (b) **Track length**: The distribution of track lengths $N_t\Delta t$ gives information on how many measurements yield to orbits of high accuracy. If the track is too short, i.e. less than 5 minutes,

the angular accuracy is too low to produce an accurate orbit even if object association is performed correctly [13].

(c) **Time between consecutive tracks**: Time between consecutive tracks of the same target object. If tracks are too close in time, they are effectively a single track. Too much apart, and we are back to the issue of bad object association. Therefore, tracks should be spaced between 15 and 45 minutes in LEO.

2.5. Simulation

In the numerical simulation environment, constellations are initialised with the true anomaly of the first satellite equal to 0. Unless otherwise specified (i.e., in coverage variability analyses), the Sun direction is assumed to be taken at the Autumn equinox. In all cases, propagation is done accordingly to averaged non-Keplerian dynamics under Earth-oblateness perturbation J_2 [14]:

$$\dot{\Omega} = -\frac{3}{2} n J_2 \left(\frac{R_e}{p}\right)^2 \cos i \tag{5}$$

$$\dot{\omega} = \frac{3}{2} n J_2 \left(\frac{R_e}{p}\right)^2 \left(2 - \frac{5}{2}\sin^2 i\right) \tag{6}$$

$$\dot{M} = n \tag{7}$$

where Ω is the right ascension of the ascending node (RAAN), ω the argument of periapsis, M the mean anomaly, n the mean motion, p the length of the semi-latus rectum, i the orbit inclination and R_e the radius of the Earth. We consider only targets of diameter equal or greater than 10 cm. Moreover, we consider Low-Earth Orbit (LEO), i.e. targets orbiting at altitudes between 400 and 2000 km.

For estimating the static metrics, we initialise 10^4 target points according to the 2024 distribution as estimated by ESA Master Software [15]. At every timestep, coverage is compute using Monte-Carlo integration [7] to approximate the expected value of Eq. 3:

$$\overline{\text{cov}_N}(t) = \sum_{\mathbf{r}_t, D_t \sim p_t} f_{v,N}(\mathbf{r}_t, D_t) \tag{8}$$

where p_t is the target position and size distribution (see Fig. 4). Simulations for daily coverage estimate have a timespan of one orbital period, as the constellation repeats itself periodically after that, while target points are fixed. To estimate coverage scalability, we assume a starting constellation of 20 satellites and 10 subsequent launches. After each new launched satellite, every satellite in the target orbit manoeuvres to redistribute at a constant angular displacement.

Simulations for dynamic metrics require more care to minimise computation time. Indeed, static simulations have time complexity $O(N_t)$, where N_t is the number of targets, while dynamic simulations have complexity $O(N_t N_k)$, where N_k is the number of timesteps. Using too few targets results in population undersampling, while using too few timesteps incurs in the risk of neglecting targets that are well tracked but sinchronised with time instant outside the time sampling. We choose simulations lasting 5 orbital periods (about 8 hours, which is the time required for the update of TLEs), with Δt = 30 s as tracks less than half a minute long do not yield accurate enough information for good tracking. We also sample 500 targets from the current known distribution of LEO targets above 10 cm. We neglect Starlink satellites as they are generally well tracked and may pollute the generalizability of the results given their high proportion in the current LEO population.

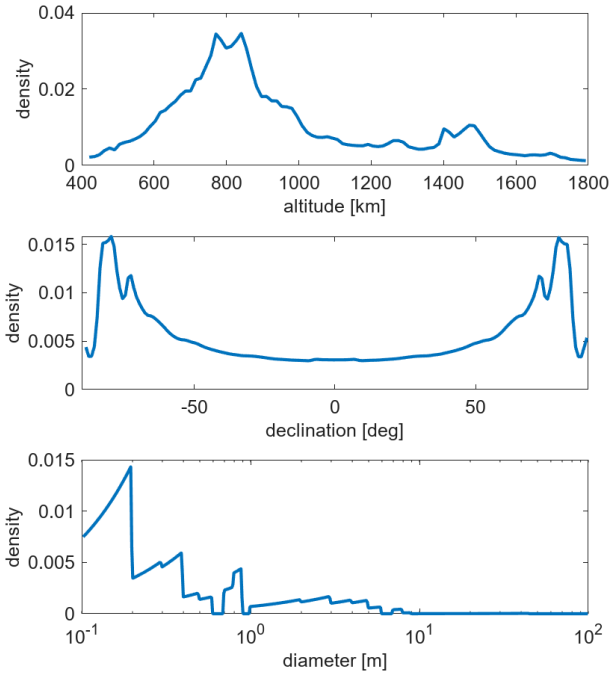

Figure 4: Target distribution in LEO as obtained with the ESA MASTER software [15]

3. RESULTS

This section summarizes and discusses the results obtained in the numerical simulations for both static and dynamic performance. Tracking performance refers to dynamic performance when considering the FOV visibility condition as discussed in Section 2.1.

3.1. Static performance

Fig. 5 shows the coverage maps for the three architectures described in Section 2.2. The coverage maps are computed for the peak target altitude of 800 km and the average target size of 70 cm. We can observe how Walker constellation yields a more even coverage, but the lower overlapping between field-of-regards (FOR) yields

a lower visibility count on average, especially at the poles where targets are more concentrated.

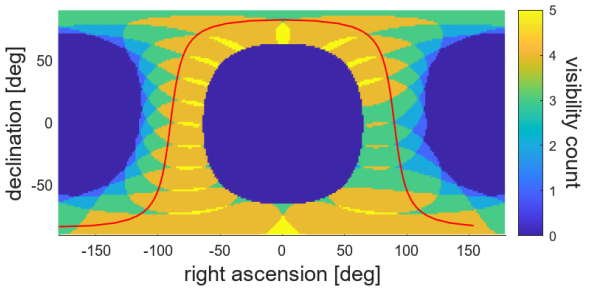

(a) Single SSO

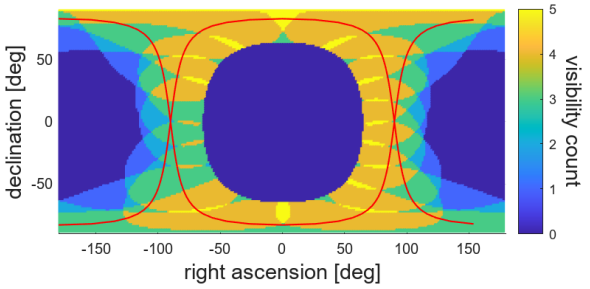

(b) Double SSO

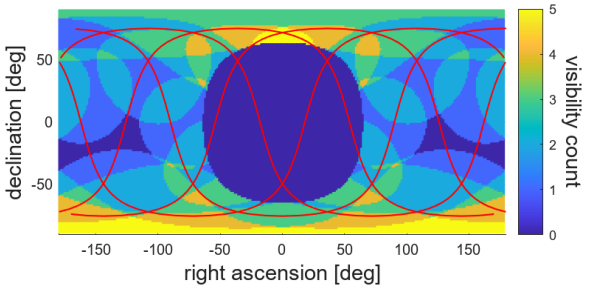

(c) Walker

Figure 5: Coverage maps for the three tested architecture as described in Section 2.2. A visibility count of 5 indicates that the corresponding point in space can be observed by at least 5 sensors. Visibility maps are computed for targets of size 70 cm at an altitude of 800 km. The red curves indicate the trajectories of the constellation. Sun direction taken at the Autumn equinox.

The time variation of the 1-fold and 3-fold coverage is shown in Fig. 6, where it is clear that the Double SSO constellation gives a superior performance thanks to the higher coverage volume compared to the single orbit. The Walker constellation is the worse one because it does not optimise for the target distribution, which is more agglutinated near the poles.

The yearly coverage variation, produced by the revolution of the Earth around the Sun, is shown in Fig. 7. We can observe the effect is very similar across the three constellations, as the highest variation effect is driven by the elevation change of the Sun, caused by the inclination of the ecliptic plane. This effect is larger for polar constellations, compensating the advantage of Sun-synchronicity.

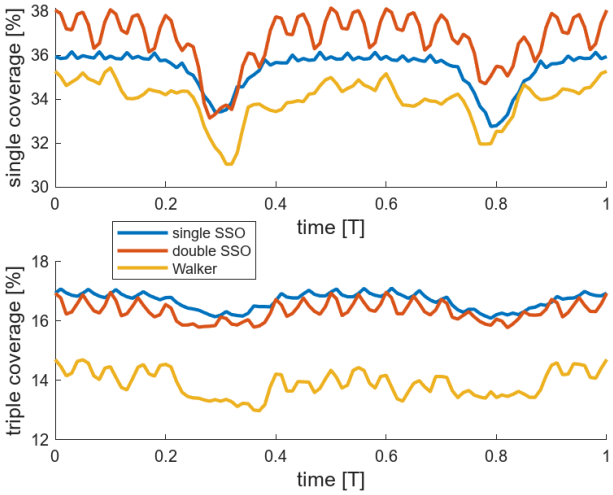

Figure 6: Time variation of 1-fold (single) and 3-fold (triple) coverage for the three constellations described in Section 2.2. T indicates the period of the constellation orbits.

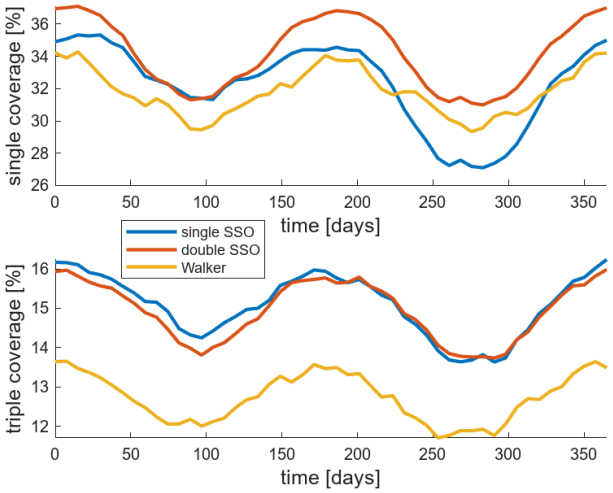

Figure 7: Yearly variation of the average 1-fold (single) and 3-fold (triple) coverage for the three constellations described in Section 2.2.

The results for coverage scalability are shown in Fig. 8. We can see that the Double SSO constellation is also the constellation with the greater capacity. Single SSO is near full capacity due to the great overlapping in the field-of-regards. On the other hand, added satellites to the Walker constellation for this range of number of satellites is too spread out to yield significant advantages. This causes a lower average marginal increase, as summarised in Table 1. Table 1 also contains a summary for the average 1-fold and 3-fold coverage computed at the Autumn equinox.

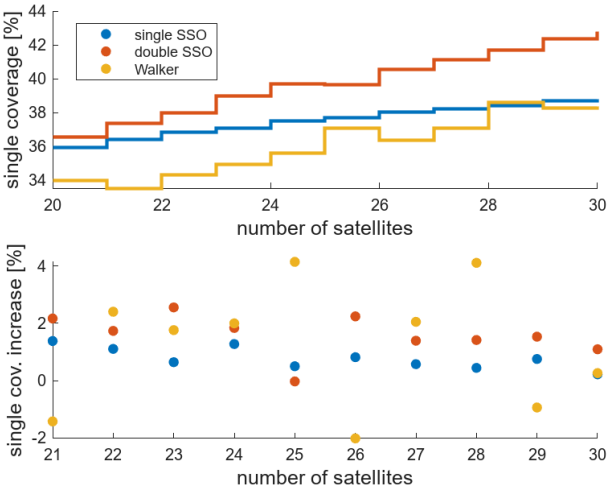

Figure 8: Above, the 1-fold (single) coverage for the three constellation architectures described in Section 2.2 as a function of the constellation satellites. Below, the marginal increase in single coverage as a function of the constellation satellites. The variability in the marginal increase is partly due to the approximation introduced by the Monte Carlo integration method and the low sampling in time. T indicates the period of the constellation orbits.

Table 1: Average 1-fold coverage, 3-fold coverage and marginal increase in 1-fold coverage for the three architectures described in Section 2.2.

Architecture	cov_1 [%]	cov_3 [%]	$\frac{\Delta \text{cov}_1}{\Delta N_s}$ [%]
Single SSO	35.6	16.8	0.7
Double SSO	36.5	16.5	1.6
Walker	33.9	13.9	1.1

3.2. Dynamic performance

Fig. 9 shows the time variation in the percentage of observed objects within one half orbital period, a metric chosen for reasons explained in Section 2.4. The Single SSO constellation is the best performing one in this case, but is closely tied with Double SSO. This suggests that having an high level of overlapping in the field-of-regards helps in intercepting a high percentage of targets.

Fig. 10 shows the distribution of track lengths and times between consecutive tracks for the Double SSO constellation. For both we can see a distribution with a double peak, suggesting targets are divided between those that are tracked for long time intervals with negligible time between consecutive tracks, and those that are tracked with more difficulties, composing the variable portion of the percentage of observed targets as shown in Fig. 9. In particular, targets with tracks separated by more than half

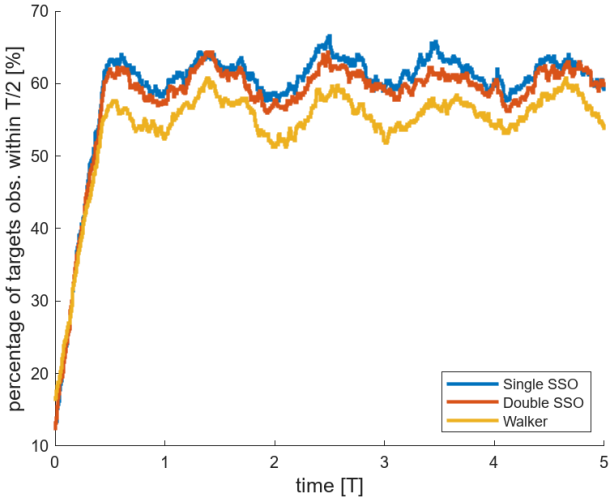

Figure 9: Percentage of objects observed at least one time within half a orbital period of the current timestep for the three architectures described in Section 2.2. T indicates the period of the constellation orbits.

a orbital period, periodically enter and exit the percentage of observed targets, justifying the general behaviour of the curve. A comparison for the three architectures is shown in Table 2, where it is shown that the Double SSO constellation is the best one in terms of median track length, while retaining a median time between tracks lower than 45 minutes, compatible with good tracking as explained in Section 2.4.

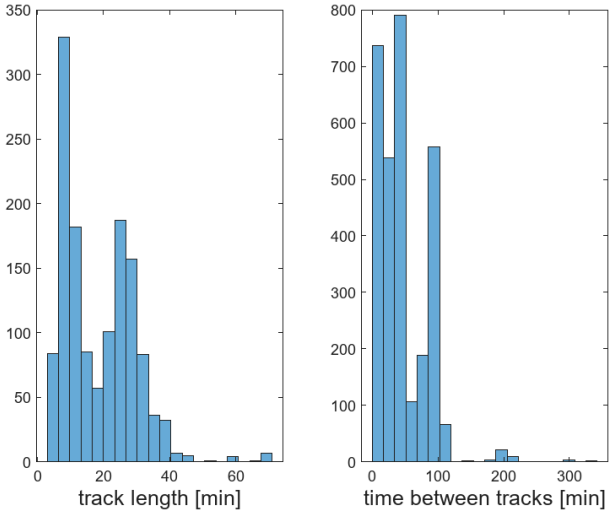

Figure 10: Distribution of track lengths and time between consecutive tracks as defined in Section 2.4 for a Double SSO constellation. About half of the targets are well-tracked with long track lengths and small time between tracks.

Table 2: Average percentage of observed targets within one half orbital period and median track lengths and time between consecutive tracks for the three architectures described in Section 2.2.

Architecture	$\overline{p_{obs}}$ [%]	$\overline{N_t \Delta t}$ [min]	$\overline{\text{tbt}}$ [min]
Single SSO	61.5	15.5	45.5
Double SSO	60.1	16.5	43
Walker	56.0	12.5	35.5

3.3. Tracking performance

As explained in Section 2.1, the previous results neglect the field-of-view condition to retrieve an upper bound for the performance of the constellation architecture as a whole. In reality, an observation is realised only when the camera is pointing to a target, and therefore the real performance can only be retrieved once a tracking strategy is defined. Fig. 11 compares the four tracking strategies described in Section 2.3 in terms of percentage of target population observed within one half orbital period. Among the three static strategies, *Radial* performs noticeably worse as the field-of-view spans a much lower subvolume of the LEO shell. *Greedy* however, despite being uncoordinated and memoryless, is almost three times more efficient than the best tracking strategy, reaching almost half of the limiting performance as retrieved in Section 3.2.

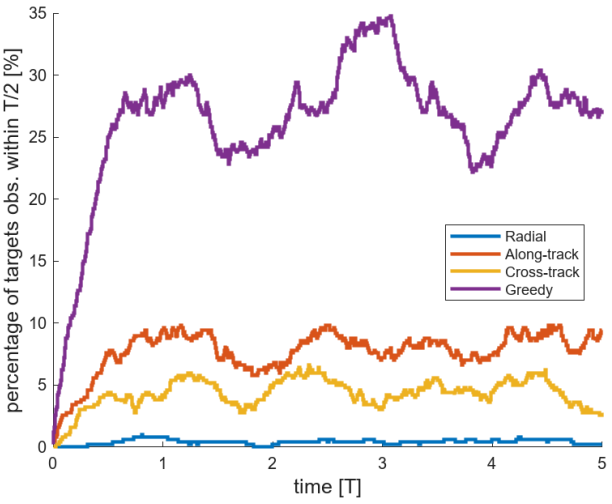

Figure 11: Percentage of objects observed at least one time within half a orbital period of the current timestep for the four tracking strategies described in Section 2.3, Double SSO constellation. T indicates the period of the constellation orbits.

A summary comparison of the four strategies is provided in Table 2, where we can observe that *Greedy* also provides the highest median track length while lowering substantially the median time between consecutive tracks, suggesting it can be used for reliable tracking of a good portion of the target population.

Table 3: Average percentage of observed targets within one half orbital period and median track lengths and time between consecutive tracks for the three tracking strategies described in Section 2.3, Double SSO constellation.

Strategy	$\overline{p_{obs}}$ [%]	$\overline{N_t \Delta t}$ [min]	$\overline{\text{tbt}}$ [min]
Radial	0.4	0.5	197.5
Along-track	8.2	6	93
Cross-track	4.5	5.5	100.5
Greedy	27.7	7.5	11.5

3.4. Dependence on limiting magnitude

In all our simulations we have assumed the limiting magnitude of the sensor is +12. This may not always be the case, especially in very low cost missions with lower performing payload. To understand the limitations of this analysis, Fig. 12 shows how the average 1-fold and 3-fold coverage vary with limiting magnitude for the Double SSO constellation (20 satellites). Despite an high decrease in performance, we can observe that even sensors in the +7 to +8 range, like star trackers [16], can provide non-negligible coverage when accounting for the actual target distribution. This suggests very low-cost Pathfinder missions may be designed to validate this mission concept.

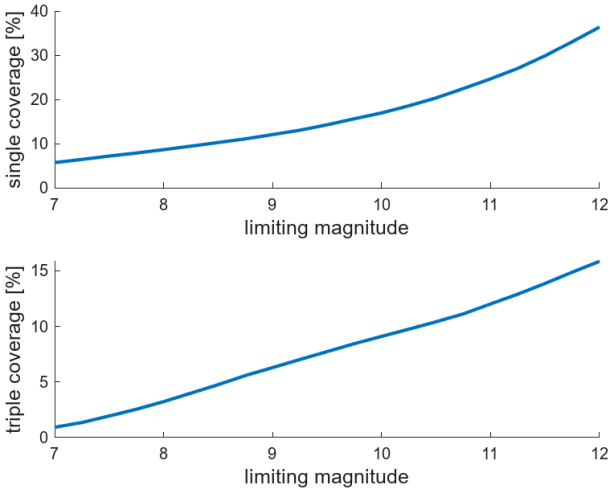

Figure 12: Average 1-fold (single) and 3-fold (triple) coverage for the Double SSO constellation as a function of the limiting magnitude of the sensor. Growth is approximately parabolic for single coverage and linear for triple coverage.

4. CONCLUSIONS

In this paper, we developed a methodology for comparing multiple network architectures for optical space-to-space surveillance. After providing suitable visibility models and restricting ourselves to a subset of reasonably well-posed constellations and tracking strategies, we defined a set of quantitative performance metric related to tracking performance. The different architectures were then tested for such metrics in a numerical simulation environment, taking into account the computational requirements of the analysis.

The results showed that for constellation of 20 to 30 observer satellites, the best architecture is a double symmetric orbit at a Sun-Synchronous inclination with a symmetry plane perpendicular to the direction of the Sun. Such a constellation strives a balance between the exploitation of the polar regions and the distribution of the field-of-regards (FOR), maximising the coverage weighted against the current satellite and debris distribution. Moreover, such a constellation also proved to be the best in terms of scalability in that range, while being competitive in the percentage of tracked orbits and the best in terms of median track quality.

Once we retrieved the upper bound for the performance of the Double SSO constellation, we tested multiple tracking strategies to understand the performance in a realistic case using narrow sensor field-of-view (FOV). The analysis showed that a tracking strategy that is uncooperative and memoryless in enough to reach almost half of the upper bound, reinforcing the feasibility of the mission concept.

Our results support the possibility of effectively using space-based sensing to complement ground-based networks for the surveillance of the Low-Earth Orbit (LEO) region. Moreover, the methodology we have developed is versatile and robust enough that can be applied to any class of space-based surveillance missions to retrieve upper bounds in performance. Lastly, the tracking results encourage further research in exploiting cooperation to maximise tracking performance while reducing the computational burden, as the choice of tracking strategy had a huge impact on the results with yet much distance from the retrieved performance upper bounds.

REFERENCES

1. ESA, (2023). Annual Space Environment Report, available at: https://www.esa.int/Space_Safety/ESA_s_Space_Environment_Report_2023
2. eoPortal, (2012). SBSS (Space-Based Surveillance System), available at: https://www.eoportal.org/satellite-missions/sbss
3. Utzmann J., Kraft S., (2023). Space-Based Optical Component (SBOC) for the ESA VISDOMS mission, Proceedings of the Advanced Maui Optical and Space Surveillance Technologies Conference
4. Hussain K. F., at al., (2025). Space-based debris trajectory estimation using vision sensors and track-based data fusion techniques, Acta Astronautica, DOI: https://doi.org/10.1016/j.actaastro.2025.01.038
5. Barles, A., Bilkhu, S., Boulnois, A. et al., (2022). Mission ORCA: Orbit Refinement for Collision Avoidance. Adv. Astronaut. Sci. Technol. 5, 149–165, DOI: https://doi.org/10.1007/s42423-022-00106-8
6. Felicetti L., Reza Emami M., (2017). Attitude coordination of multiple spacecraft for space debris surveillance, Advances in Space Research, DOI: https://doi.org/10.1016/j.asr.2016.12.012
7. D'Anniballe A., Felicetti L., Hobbs S., (2025). Preliminary analysis and design of an optical space surveillance and tracking constellation for LEO coverage, Acta Astronautica, DOI: https://doi.org/10.1016/j.actaastro.2025.02.019
8. Rainbow J., (2024). Aerospacelab to build debris-tracking satellite for Vyoma, available at: https://spacenews.com/aerospacelab-to-build-debris-tracking-satellite-for-vyoma/
9. Hejduk M. D., (2011). Specular and Diffuse Components in Spherical Satellite Photometric Modeling, Proceedings of the Advanced Maui Optical and Space Surveillance Technologies Conference
10. Clemens S., (2019). On-Orbit Resident Space Object (RSO) Detection Using Commercial Grade Star Trackers
11. Wertz J. R., (2009). Orbit and Constellation Design and Management, Space Technology Library, Vol. 13
12. D'Anniballe A., (2022). Catalogue initialization : assessing optical tracklet to tracklet association methods
13. Dolado J. C., Yanez C., Anton A., (2016). On the Performance Analysis of Initial Orbit Determination Algorithms, Proceedings of the 67th International Astronautical Congress (IAC)
14. Vallado D. A., (2013). Fundamentals Of Astrodynamics And Applications, Space Technology Library
15. ESA. MASTER, available at: https://sdup.esoc.esa.int/
16. Filho J., et al., (2023). Satellite Star Tracker Breadboard with Space Debris Detection Capability for LEO, Journal of Physics: Conference Series, DOI: https://doi.org/10.1088/1742-6596/2526/1/012119